Effects of Ultrasonic Exposure Parameters on Myocardial Lesions Induced by High-Intensity Focused Ultrasound

Kana Fujikura, MD, Ryo Otsuka, MD, Andrew Kalisz, MSEE, Jeffrey A. Ketterling, PhD, Zhezhen Jin, PhD, Robert R. Sciacca, EngScD, Charles C. Marboe, MD, Jie Wang, MD, PhD, Robert Muratore, PhD, Ernest J. Feleppa, PhD, Shunichi Homma, MD

Objective. This study evaluated variables relevant to creating myocardial lesions using high-intensity focused ultrasound (HIFU). Without an effective means of tracking heart motion, lesion formation in the moving ventricle can be accomplished by intermittent delivery of HIFU energy synchronized by electrocardiographic triggering. In anticipation of future clinical applications, multiple lesions were created by brief HIFU pulses in calf myocardial tissue ex vivo. ***Methods.*** Experiments used f-number 1.1 spherical cap HIFU transducers operating near 5 MHz with in situ spatial average intensities of 13 and 7.4 kW/cm^2 at corresponding depths of 10 and 25 mm in the tissue. The distance from the HIFU transducer to the tissue surface was measured with a 7.5-MHz A-mode transducer coaxial and confocal with the HIFU transducer. After exposures, fresh, unstained tissue was dissected to measure visible lesion length and width. Lesion dimensions were plotted as functions of pulse parameters, cardiac structure, tissue temperature, and focal depth. ***Results.*** Lesion size in ex vivo tissue depended strongly on the total exposure time but did not depend strongly on pulse duration. Lesion width depended strongly on the pulse-to-pulse interval, and lesion width and length depended strongly on the initial tissue temperature. ***Conclusions.*** High-intensity focused ultrasound creates well-demarcated lesions in ex vivo cardiac muscle without damaging intervening or distal tissue. These initial studies suggest that HIFU offers an effective, noninvasive method for ablating myocardial tissues to treat several important cardiac diseases. ***Key words:*** electrocardiographic triggering; focused ultrasound surgery; high-intensity focused ultrasound; myocardial ablation.

Abbreviations
ECG, electrocardiographic; HIFU, high-intensity focused ultrasound; I_{SA}, spatial average intensity; LV, left ventricular; PBS, phosphate-buffered saline; RF, radio frequency; RV, right ventricular

Received January 5, 2006, from Columbia Presbyterian Medical Center, New York, New York USA (K.F., R.O., Z.J., R.R.S., C.C.M., J.W., S.H.); and Riverside Research Institute, New York, New York USA (A.K., J.A.K., R.M., E.J.F.). Revision requested February 16, 2006. Revised manuscript accepted for publication July 3, 2006.

We acknowledge the insight, inspiration, and encouragement of the late Frederic L. Lizzi, EngScD. We thank Christopher J. Vecchio, PhD, and Michael K. Knauer for engineering contributions. This research was supported in part by Bioengineering Research Partnership grant CA 084588 from the National Cancer Institute and the National Heart, Lung, and Blood Institute and a scholarship to Dr Fujikura from the Japanese Society of Echocardiography.

Address correspondence to Kana Fujikura, MD, Department of Biomedical Engineering, Columbia University, Columbia Presbyterian Medical Center, 622 W 168th St, VC12-234, New York, NY 10032 USA.
E-mail: kf2113@columbia.edu

Two prevailing techniques currently are used to ablate cardiac ventricular tissue for treatment purposes: radio frequency (RF) ablation[1] and alcohol ablation.[2] The former technique is applied to the treatment of patients with arrhythmia, whereas the latter treats patients with hypertrophic obstructive cardiomyopathy accompanied by severe symptoms. Both ablative techniques make use of catheterization. Radio frequency ablation is used to dis-

rupt aberrant conduction pathways that cause arrhythmias; RF ablation creates a hemispheric lesion that, depending on the location of the region to be treated, also may cause collateral damage in peripheral tissue. Alcohol ablation is used to stimulate blood flow in the septal arteries; ethanol causes an infarction, which results in scarring, thinning of the septal wall, and improved blood flow. Ablating regions close to or on the epicardium can be problematic with RF ablation because of insufficient penetration of RF energy (eg, resulting from a large distance between the endocardial catheter contact point to critical areas of tachycardia circuits).[3] Alcohol ablation can be problematic because of difficulties in selecting the proper feeding artery of the hypertrophic septum.[4]

In comparison, the high-intensity focused ultrasound (HIFU) technique described in this article can potentially overcome some of the limitations of RF and alcohol ablation. First proposed by Lynn et al[5] in 1942 and further developed by Fry's group[6–8] in the 1950s, therapeutic HIFU research has led to clinical therapies in urology, ophthalmology, and oncology.[9–16] Currently, commercial units are available that provide HIFU treatment for atrial fibrillation.[17,18] Although several investigators have worked on cardiac ventricular applications of HIFU[19–25] in the past, studies of optimal ways to synchronize lesion formation with cardiac cycles have yet to be made. High-intensity focused ultrasound can be applied in a noninvasive or minimally invasive manner, and it is capable of ablating subsurface tissue via thermal and cavitational mechanisms without causing injury to intervening tissue.[6] However, obstacles to using HIFU for cardiac applications are the motion of the heart and the complexity of the heart architecture. This article addresses means of quantitatively assessing optimal ways of delivering HIFU in the presence of heart motion that will be encountered in future in vivo studies.

The purpose of the study described in this article was to investigate and gain insight into the effects of the following factors on ex vivo lesion production: (1) pulse parameters (ie, pulse duration and pulse-to-pulse interval), (2) depth in cardiac tissue, and (3) initial tissue temperature. These insights were necessary to enable us to assess the feasibility of future HIFU applications for clinical use and to elucidate the characteristics of ex vivo myocardial lesions. This article describes our recent studies of synchronizing lesion-generating pulses with a simulated electrocardiographic (ECG) signal. We found that brief HIFU pulses could be delivered repeatedly to a small, well-defined region of myocardium at a fixed point in the cardiac cycle using rectangular pulses simulating an ECG signal as a synchronizing trigger. Electrocardiographic signals are used by many investigators to select the desired portion of the cardiac cycle.[26] For example, multiple brief HIFU pulses could be delivered at a given point in the end-diastolic phase (ie, before the systolic phase begins) when cardiac motion is minimal. Therefore, by estimating the dependence of lesion characteristics on various parameters of insonification during exposures that are synchronized to the heart cycles, this technique may overcome one of the major obstacles in using HIFU for cardiac applications: the inherent motion of the contracting heart.

Materials and Methods

Transducers

Two HIFU transducers were used; they are shown in Figure 1. Table 1 describes the characteristics of the transducers, referred to as transducers 1 and 2. The 2 transducers had similar f-numbers (ratio of focal length to aperture) and focal zone intensities. Transducer beam patterns were visually inspected for uniformity with a custom-built laboratory schlieren optical system. Radiated acoustic powers were estimated (with an uncertainty of 5%) from radiation force measurements using a flat, absorbing target watt meter.[27–29] During subsequent insonification of ex vivo tissue, the in situ spatial average intensity (I_{SA}, the intensity spatially averaged over the half-power width of the focal plane beam), was estimated, assuming a tissue-attenuation coefficient of 0.35 dB/(MHz · cm)[30,31] and linear propagation in the tissue. Nonlinear propagation at high power levels is expected to introduce higher-frequency harmonics, which increase the uncertainty of I_{SA}. The transducers contained custom 50-Ω matching networks and were excited by continuous sinusoidal waves that were generated with an Agilent 33250A function generator (Agilent Technologies, Inc, Palo Alto, CA) and

amplified using a 2100L linear amplifier (ENI, Rochester, NY).

Transducer 1 (CST-100T; Sonocare Inc, Upper Saddle River, NJ) was a 4.67-MHz spherical cap transducer with an 80-mm diameter and 90-mm focal length, and its acoustic power was 46 W. We focused the HIFU beam inside the tissue sample at a depth of 10 or 25 mm below the surface. Table 1 only shows parameters for a tissue penetration depth of 10 mm, which is consistent with most of our experiments. The estimated in situ I_{SA} values at depths of 10 and 25 mm from the surface were 13 and 7.4 kW/cm^2, respectively, for this transducer. To achieve acoustic coupling to tissue specimens, transducer 1 was housed within a 65-mm acrylic resin cone filled with degassed water and capped at the distal end with a thin latex membrane. The ellipsoidal –3-dB focal region of this transducer had an axial length of 3.0 mm and a diameter of 0.36 mm, as shown in the schlieren photograph of Figure 2. A 13-mm-diameter A-mode transducer with a nominal center frequency of 7.5 MHz was contained within a hole in the center of the treatment transducer. The A-mode beam was coaxial and confocal with the HIFU beam. The distance between the HIFU transducer and the tissue surface was measured using A-mode echoes to accurately place the focus of the HIFU beam at a known depth within the tissue specimens.

Transducer 2 (Sonic Concepts, Woodinville, WA) was a spherical cap transducer with a 33-mm diameter and a 35-mm focal length; it operated at a frequency of 5.075 MHz. A 10-mm-diameter A-mode transducer (7.5 MHz) was inserted through a hole in the center of the therapy transducer. The acoustic power of transducer 2 was 37 W. The in situ I_{SA} values for this transducer were estimated to be 13 kW/cm^2 at a tissue depth of 10 mm and 7.4 kW/cm^2 at a tissue depth of 25 mm. The ellipsoidal half-power focal region of this transducer was approximately 0.32 mm in diameter and 2.0 mm in axial length.

Experimental Setup

The experimental setup is illustrated in Figure 3. Degassed phosphate-buffered saline (PBS) was maintained at 23°C or 37°C. The left ventricular (LV) free walls, including epicardium, of calf hearts were cut into rectangular blocks with

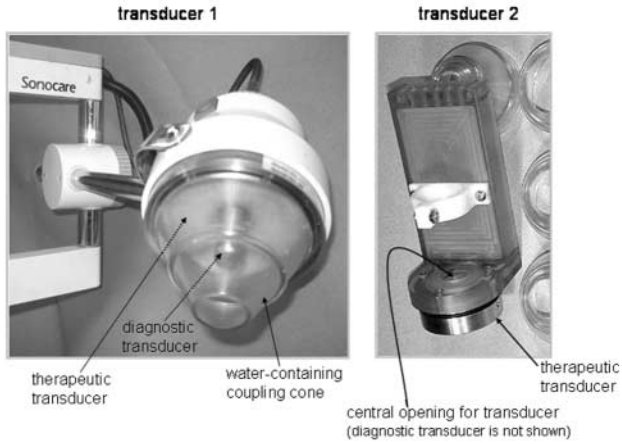

Figure 1. High-intensity focused ultrasound transducers. Detailed transducer specifications are described in Table 1.

dimensions of approximately 3 to 6 cm in length. Each sample was typically between 2.5 and 3 cm thick. The specimens were degassed and placed in a PBS bath, and the bath was then placed in a water tank to maintain the desired temperature using an electric heater (1112A; VWR International, West Chester, PA). The temperature of the tissue was monitored using a 1.7-mm needle thermocouple probe (HH506R; Omega Engineering Inc, Stamford, CT). The tip of the transducer coupling cone was placed in the PBS bath, and HIFU exposures were conducted as described below.

High-intensity ultrasound was focused 10 or 25 mm below the epicardial surface of the sample LV free wall or in the septum. Lesions were created in several different regions of each sample by moving the transducer approximately 1 cm laterally between exposures. High-intensity focused ultrasound exposures were controlled using custom-programmed LabVIEW-based software (LabVIEW 7.0; National Instruments, Austin, TX)

Table 1. High-Intensity Focused Ultrasound Transducer Specifications

Specification	Transducer 1	Transducer 2
Frequency, MHz	4.67	5.075
Diameter, mm	80	33
Focal length, mm	90	35
f-number	1.1	1.1
I_{SA}, kW/cm^2*	13	13
Diagnostic transducer	A-mode	A-mode

*At a tissue depth of 10 mm.

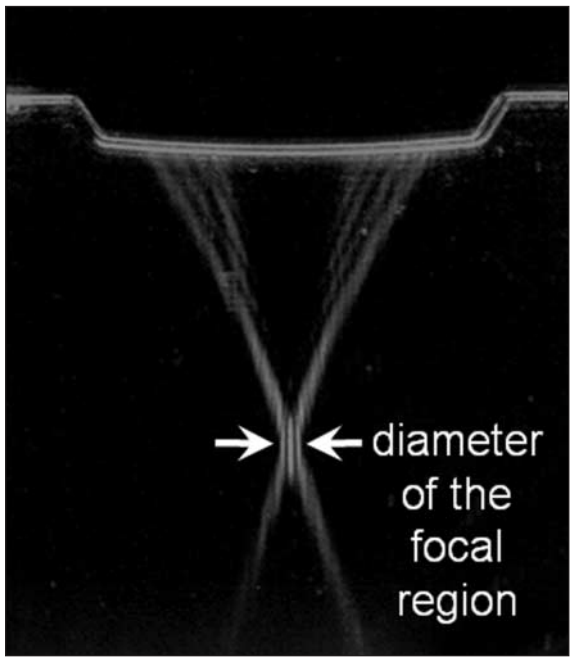

Figure 2. Schlieren image of the beam from transducer 1. The beam has a conical shape and converges to an ellipsoidal focal region with a diameter of 0.36 mm at the –3-dB point at a range of 90 mm.

that triggered externally generated rectangular pulses intended to provide a highly simplified simulation of an ECG signal. A diagram of the HIFU trigger pulse pattern is shown in Figure 4. Individual pulse durations were either 0.2 or 0.3 seconds, and the pulse-to-pulse interval (ie, the time from the end of one pulse to the start of the next one) was 4.0 seconds.

After HIFU exposures, the fresh, unstained tissue was dissected carefully to make the lesion visible at its maximum length and width. Lesion length and width then were measured manually with a Sylvac-Fawler (Newton, MA) digital vernier caliper (accuracy, ±0.03 mm) and plotted as a function of total exposure, that is, the product of the individual pulse duration and the number of pulses delivered.

Figure 3. Schematic diagram of the HIFU lesion-creating system. A tissue sample was mounted on a sound-absorbing material (10-mm-thick viscoelastic polymer, specific acoustic impedance, $Z = 1.5 \times 10^6$ rayl, which is identical to that of water [Sorbothane; Sorbothane Inc, Kent, OH]) and placed in a container filled with degassed PBS. The container was immersed in a water bath with the temperature kept at 37°C.

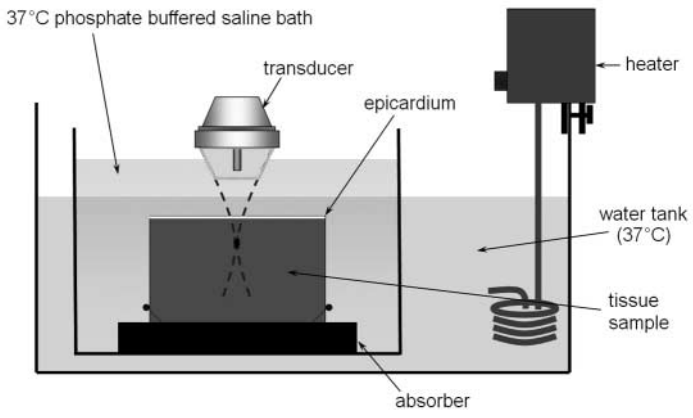

Comparison Study of Fresh Versus Stored Specimens

Because stored specimens were easier to obtain and less expensive than fresh specimens, we preferred to use them. However, we needed to verify that results obtained with stored and fresh material would be equivalent. Therefore, we performed limited studies to determine whether storing tissue affected results. Fresh calf hearts were collected immediately after slaughter and were transported to the laboratory. These were compared with vacuum-packed calf hearts that were stored at 4°C and cut into rectangular blocks having the same dimensions as those of the stored hearts described above. The temperature of the tissue samples was raised gently from 4°C to 37°C in PBS over 30 minutes. For those comparisons, transducer 1 was focused 10 mm below the epicardial surface of the rectangular block, and two to six 0.3-second pulses were delivered at 4-second intervals. Eight to 16 lesions were created for each set of pulses (fresh, n = 40; stored, n = 31).

Specimens then were fixed in 10% formalin and embedded in paraffin. Subsequently, tissue blocks were cut into 5-μm thin sections, stained with Masson trichrome stain, and examined by light microscopy. Light microscope examinations showed that the size and shape of the lesions were statistically the same in stored and fresh samples for identical exposure conditions.

Multiple Factor Studies

The factors that we evaluated are summarized in Table 2.

Pulse Parameter Studies

Two pulse durations were used with a single interpulse (ie, pulse-to-pulse) period of 4 seconds (as described above) to assess the effects of pulse duration on lesion size. As previously described, transducer 1 was positioned to focus at a depth of 10 mm below the surface of the LV free wall. The sample temperature was maintained at 37°C. In these studies, the HIFU beam was activated for pulse durations of 0.2 or 0.3 seconds. Our previous experience showed that a minimum time of 0.2 seconds was required for lesion production, and studies by Tridandapani et al[26] showed that a quiescent period of approximately 0.3 seconds occurs in diastole. Therefore, HIFU pulses of 0.2 or 0.3 seconds were delivered multiple times with a 4-second period. The number of HIFU pulses delivered to each lesion varied from 2 to 10 and affected the total exposure time, which was the number of pulses × pulse duration. Six or 7 lesions were created for each pulse duration and for each number of pulses (n = 65). Lesion length and width were measured using a vernier caliper, and average values were plotted as a function of total exposure.

Lesions then were created using a pulse-to-pulse interval of 0.8 or 4.0 seconds with a fixed pulse duration of 0.2 seconds while the number of pulses was varied between 2 and 10. Seven to 10 lesions were created for each number of pulses and each pulse-to-pulse interval (n = 92). Lesion length and width were measured using a vernier caliper, and average values were plotted as a function of the number of pulses; the lesion dimensions then were compared for each pulse-to-pulse interval used.

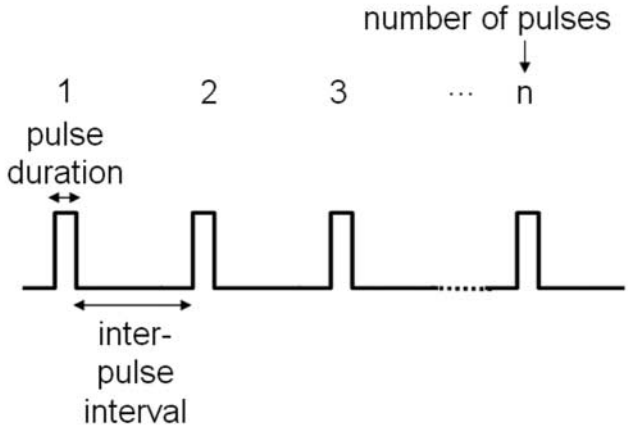

Figure 4. Simple scheme for simulating ECG triggering. High-intensity focused ultrasound exposures of 0.2- or 0.3-second durations were repeated with a fixed interpulse interval of 4 seconds.

Cardiac Structure Studies

To assess the effect of tissue attenuation on lesion formation inside the tissue, transducer 2 was set to focus either at 10 or 25 mm below the surface of the LV free wall. The sample temperature was maintained at 37°C. A series of 0.3-second pulses were applied using a pulse-to-pulse interval of 4 seconds. The number of pulses was 10, 15, or 20 for both focal depths. Five to 8 sites were exposed using each number of pulses (n = 67). The lesion dimensions were measured using a vernier caliper, and average values were plotted as a function of the number of pulses.

Lesions also were made in the LV septum through the overlying right ventricular (RV) free wall with attached epicardium using transducer 2. The transducer was set to focus 25 mm below the epicardium to focus within the LV septum. Then, 0.3-second pulses were applied at a pulse-

Table 2. Summary of the Protocols

	Pulse Parameter Studies		Cardiac Tissue Studies		
Parameter	Pulse Duration	Interpulse Interval	Depth From Surface	Formation Through RV Free Wall	Tissue Temperature Studies
Transducer	1	1	2	2	2
Pulse duration, s	0.2 or 0.3	0.2	0.3	0.3	0.3
Interpulse Interval, s	4	0.8 or 4	4	4	4
Depth from surface, mm	10	10	10 or 25	25	10
Focus tissue	LV free wall	LV free wall	LV free wall	LV or septum	LV free wall
Baseline temperature, °C	37	37	37	37	37 or 23
Samples, n	65	85	36	40	48

to-pulse interval of 4 seconds. The number of pulses was 20, 25, or 30. The same exposure parameters were applied to a sample of the LV free wall at the same focal depth. The sizes of lesions created in the septum through the RV free wall were compared with those made in the LV free wall. Five to 8 sites were exposed using each number of pulses (n = 51). The lesion length and width were manually measured with a vernier caliper, and average values were plotted as a function of the number of pulses.

Tissue Temperature Studies

The focal point for transducer 2 was set at a depth of 10 mm below the epicardium within the LV free wall. The temperatures of the tissue and degassed PBS bath were set at either 23°C (room temperature) or 37°C. The typical time for raising the temperature from room temperature to 37°C was 30 min. A series of pulses with a 0.3-second duration were delivered 5, 10, 15, or 20 times for tissue at 37°C and then for tissue at 23°C. The pulse-to-pulse interval was set to 4 seconds. Five to 8 sites were exposed at the above number of pulses (n = 68). Average lesion length and width were individually compared between the 2 temperature groups.

Statistics

Results are expressed as mean values ± 1 SD. Data were analyzed using SAS 8.2 software (SAS Institute Inc, Cary, NC). The comparison between the lesions created in fresh and stored samples was done using analysis of covariance. In multiple-factor studies, the effects of different experimental conditions on lesion length and width were assessed using analysis of variance or analysis of covariance whenever appropriate. Statistical significance was defined as a $P < .01$.

Results

Comparison Study of Fresh Versus Stored Specimens

Analysis of covariance was used for comparing the length and width of the lesions created by HIFU in fresh versus stored samples. The length of HIFU lesions as a function of the number of pulses and specimen type was described by the following equation:

$$L = 3.17 + 1.14\,N - 0.52\,G_s,$$

where L was the lesion length in millimeters; N was the number of pulses; and G_s was the group: $G_s = 1$ for fresh samples and 0 for stored samples. $P = .09$ for its coefficient, which showed that there was no statistical difference in lesion length between fresh and stored samples. The width of HIFU lesions as a function of the number of pulses and the specimen type was described by the following equation:

$$W = 0.64 + 0.32\,N - 0.17\,G_s,$$

where W was the lesion width in millimeters. $P = .06$ for the group coefficient. The residual quantile-quantile plots indicated that assumption of a gaussian error distribution for L and W was reasonable. Overall, the size of the HIFU lesions created in fresh tissue samples could be estimated from the size of the HIFU lesions created in stored tissue samples vacuum packed at 4°C for a few days. On the basis of this result, we used more easily obtained stored tissue samples for the remainder of our studies.

Figure 5A illustrates the gross appearance of lesions formed during the pulse duration study. These lesions were well demarcated and surrounded by histologically normal tissue. Light microscope views of a histologic section of an HIFU lesion are shown in Figure 5, B and C. The HIFU lesions were clearly defined, teardrop-shaped, hyperchromatic areas with visible central disruption and irregular loss of tissue. The tissue in the path of the HIFU beam, but outside the focal region, was entirely intact. The HIFU dose was set to cause damage only in the focal region. At the focus, the intensity was high enough to produce a temperature rise sufficient to cause rapid cell death, but outside the focal region, the rise was not sufficient to be lethal. This effect has been reported by other investigators.[32]

Multiple-Factor Studies

Pulse Parameter Studies

Lesion length and width increased linearly with total exposure time for 0.2- and 0.3-second pulse durations (Figure 6). Analysis of covariance was used for comparing the different effects of 0.2-

versus 0.3-second pulses on lesion length and width after adjusting the number of pulses. The length of HIFU lesions was described by the following equation:

$$L = 3.98 + 3.40\ T - 0.34\ G_t,$$

where T was the total exposure time in seconds, and G_t was the group: $G_t = 0$ for 0.2-second pulses and 1 for 0.3-second pulses; $T = N\ t$, where N was the number of pulses, and t was the pulse duration, that is, 0.2 or 0.3 seconds. $P = .37$ for the group coefficient, which indicated that no significant difference in lesion length was shown for 0.3- versus 0.2-second pulses. The width of HIFU lesions was described by the following equation:

$$W = 0.51 + 0.89\ T + 0.34\ G_t.$$

$P = .001$ for the group coefficient, which indicated that a pulse duration of 0.3 seconds produced a significantly wider lesion than was produced by a pulse duration of 0.2 seconds. Here again, the residual quantile-quantile plots indicated that a gaussian error distribution assumption for L and W was reasonable.

Figure 7 shows the lesion length and width plotted as a function of the number of pulses for 0.8- and 4-second pulse-to-pulse intervals. The lengths of the lesions were similar for 2, 4, 6, and 8 pulses and remained similar at 10 pulses ($P = .02$). Lesion width seemed greater for an 0.8-second pulse-to-pulse interval than a 4-second interval for 4, 6, 8, and 10 pulses; however, the difference still was statistically significant ($P < .01$ in all cases).

Cardiac Structure Studies

Figure 8 shows the lesion length and width plotted as a function of the number of pulses for lesions created at focal depths of 10 and 25 mm from the cardiac surface. The lesion length and width were significantly larger at a depth of 10 mm compared with lesions created at a depth of 25 mm with 10, 15, and 20 pulses ($P < .0001$ in all cases). These marked differences almost certainly are a manifestation of differences in beam attenuation.

The lesion length and width in the cardiac septum exposed through the overlying RV free wall are shown in Figure 9 as a function of the number of applied pulses. The length and width of the lesions tended to be smaller in the septum than in the LV free wall, but the differences generally were not statistically significant ($P > .02$).

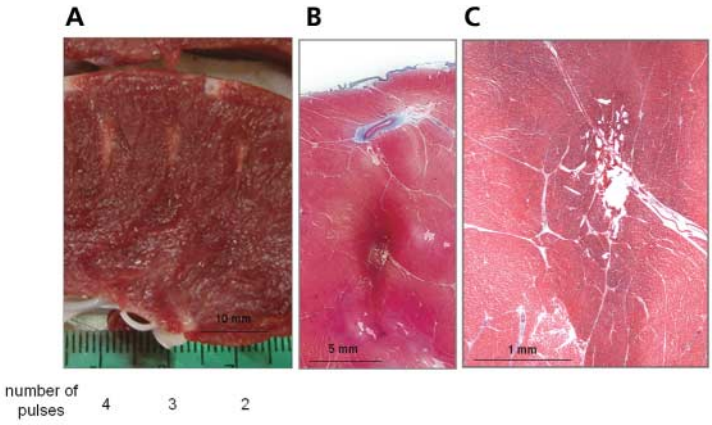

Figure 5. A, Typical cross section of lesions created in fresh ex vivo tissue using transducer 1 (pulse duration, 0.3 seconds; pulse-to-pulse interval, 4 seconds). The number of HIFU pulses used to create each lesion is shown in Figure 6. **B** and **C**, Trichrome-stained HIFU lesion shown at different magnifications. The lesions are clearly defined, teardrop-shaped, hyperchromatic areas with visible central disruption and irregular loss of tissue. Tissue in the path of the HIFU beam, but outside the focal region, appears to be entirely intact.

Tissue Temperature Studies

The effects of tissue temperature on lesion length and width are shown in Figure 10 as a function of the number of pulses. Lesion lengths at 23°C were significantly smaller than those at 37°C for 5, 10, 15, and 20 pulses ($P = .03$; $P = .002$;

Figure 6. Lesion dimensions for HIFU pulses applied multiple times with individual pulse durations of 0.2 or 0.3 seconds. The average length (**A**) and width (**B**) of the lesions are shown as a function of total exposure time for both 0.2-second (circles) and 0.3-second (squares) pulse durations. **A**, $y_{length} = 3.80 + 3.40\ x_{total\ time} - 0.34$ group; circles indicate group = 0; and squares, group = 1. **B**, $y_{width} = 0.51 + 0.89\ x_{total\ time} + 0.34$ group; circles indicate group = 0; and squares, group = 1. Error bars in Figures 6–10 represent ±1 SD.

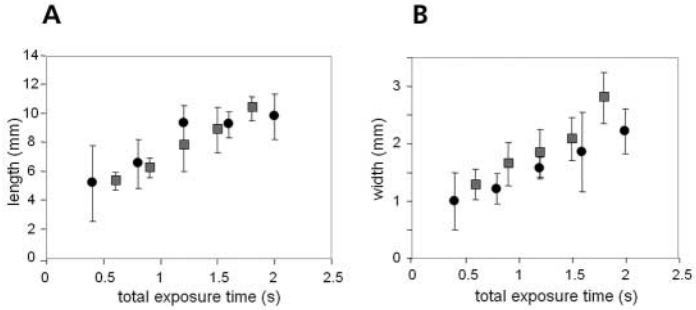

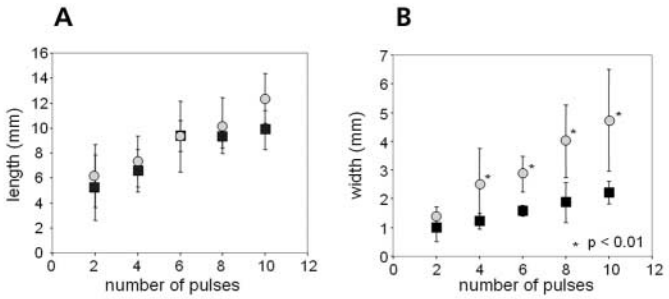

Figure 7. Effects of different pulse-to-pulse intervals. The average lesion length (**A**) and width (**B**) were plotted as a function of the number of pulses for pulse-to-pulse intervals of 0.8 seconds (circles) and 4 seconds (squares).

$P < .0001$; and $P < .0001$, respectively, by analysis of variance). Lesion widths at 23°C were significantly smaller than those at 37°C for 15 and 20 pulses ($P < .0001$ for both).

Discussion

Comparison Study of Fresh Versus Stored Specimens

This introductory study suggests that using stored specimens provides meaningful results from which ex vivo effects can be inferred. Tissue necrosis (autolysis) can be discerned by a variety of histochemical stains and has been shown to start within 2 to 3 hours after the suspension of blood flow.[33] We considered that outgassing and gas production associated with tissue necrosis and exposure to air might cause microbubbles to develop within tissue soon after an animal is killed. Degassing might not remove all the bubbles completely from stored tissue samples or even from fresh material. Because microbubbles increase the cavitational effect of HIFU, a larger lesion would be expected to result when a sample contains more microbubbles (eg, if it is stored for a greater time before exposure).[34] However, microbubbles that exist in the path of the HIFU beam before it reaches the focal point attenuate the HIFU energy and decrease the size of the HIFU lesion. Therefore, these phenomena might counteract each other or might be small effects in the range of exposure parameters that we tested with regard to the creation of HIFU lesions in our study.

Figure 8. Average lesion length (**A**) and width (**B**) plotted as a function of the number of pulses for focal depths of 10 mm (circles) and 25 mm (squares) below the surface. The length and width were significantly different between the lesions created at 10 and 25 mm for 10, 15, and 20 pulses.

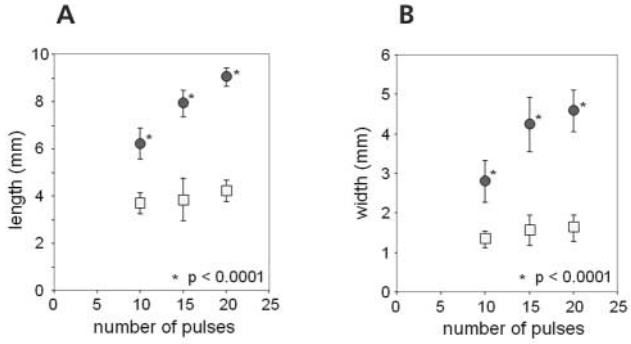

Pulse Parameter Studies

The first general factor we investigated was pulse parameters: the duration of the short HIFU pulses and the interval between those pulses. These two parameters have a direct bearing on temperature elevations and cavitational effects, which in turn affect the size of the HIFU lesion.

As the interval between HIFU exposures decreases, less time is available for conduction to remove heat from the insonified region. As a consequence, reducing the interval between successive thermal ablations increases the temperature elevation in the insonified region.

Temperature elevation and cavitational effects can work hand in hand. The deposition of acoustic energy at the focal point causes a temperature elevation and thus creates thermal ablation, and a rise in temperature has been shown to generate microbubbles.[30] In turn, the microbubbles might enhance the destruction of tissue by means of cavitation.

The effect of pulse durations of 0.2 and 0.3 seconds were evaluated using pulse-to-pulse intervals of 0.8 and 4.0 seconds. In clinical cardiac ablation applications, HIFU is easier to target by insonification during the brief end-diastolic phase when heart motion is minimal. The duration of the end-diastolic phase varies as a function of the heart rate. In planning exposures near end diastole, a key issue is the relative importance of each short pulse compared with the total exposure time. In our studies of this topic, the pulse duration was set to either 0.2 or 0.3 seconds, and lesion length and width were evaluat-

ed as a function of total exposure time. For both pulse durations, the lengths of HIFU lesions were statistically similar; however, lesion widths were significantly different as described above and shown in Figure 6. One possible explanation for the low *P* value of the width (Figure 6B) is the relatively large separation between the data points of 1.8 and 2.0 seconds. These results show that multiple HIFU exposures with a duration of 0.2 or 0.3 seconds can produce lesions in vitro, and these observations provide a starting point for studies of effects in vivo.

The effect of different pulse-to-pulse intervals, 0.8 and 4 seconds, was evaluated for 0.2-second pulse durations using the same total exposure for both intervals. As shown in Figure 7, 0.8-second pulse-to-pulse intervals created significantly wider lesions than did 4-second intervals. The 4-second intervals certainly allowed more time for the tissue to cool between pulses than was allowed by 0.8-second intervals. Because blood flow causes faster tissue cooling in vivo than what occurred in our experiments, we think that the in vivo lesion size will more closely mimic our experiments that used 4-second pulse-to-pulse intervals. Furthermore, because respiration also alters the position of the heart, synchronization may be required not only with the heartbeat but also with respiration. Choosing a 4-second pulse-to-pulse interval can be expected to facilitate this dual synchronization.

Cardiac Tissue Studies

The second general factor we investigated was the effect of attenuation in cardiac tissue. We evaluated the effect of lesion depth within the myocardium because attenuation in the LV tissue reduces the in situ intensity at the focal point. This consideration is clinically relevant because structures that trigger arrhythmias can be located at any depth within the myocardium from the endocardial to the epicardial side. As described above, an additional potential application for future HIFU treatments is LV septal ablation for hypertrophic cardiomyopathy with severe obstruction of the LV outflow tract. For the HIFU beam to reach the septum, the minimal distance to the septum would be obtained by focusing the HIFU beam through the thinner RV free wall and smaller RV cavity rather than through the thicker LV free wall and the larger LV cavity. The cavity of the RV includes the endocardium, papillary muscles, and tendons. The in situ intensity at the focal point through these structures may differ from the intensity through the relatively homogeneous LV free wall.

Our studies of depth effects compared 3 sets of numbers of pulses, 10, 15, and 20, at focal points that were 10 and 25 mm below the tissue surface. The same acoustic power from the transducer was used in all cases. Lesion length and width were significantly smaller at the deeper site for all numbers of HIFU pulses (Figure 8). To produce a fixed size lesion, HIFU power would need to increase according to the depth of the target tissue, that is, to compensate for attenuation, as expected.

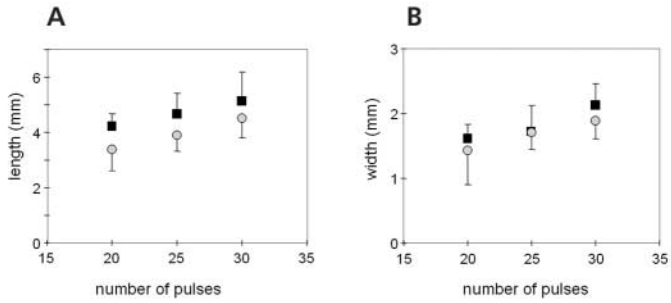

Figure 9. Average length and width of HIFU lesions created at a depth of 25 mm from the surface in the LV free wall (squares) and the septum through the RV (circles). Both average length (**A**) and average width (**B**) in the septum tended to be smaller than those in the LV free wall.

Figure 10. Average length (**A**) and width (**B**) of HIFU lesions created using different tissue temperatures, 37°C (squares) and 23°C (circles), plotted as a function of the number of pulses. The length was significantly different for 5, 10, 15, and 20 pulses, and the width was significantly different for 15 and 20 pulses.

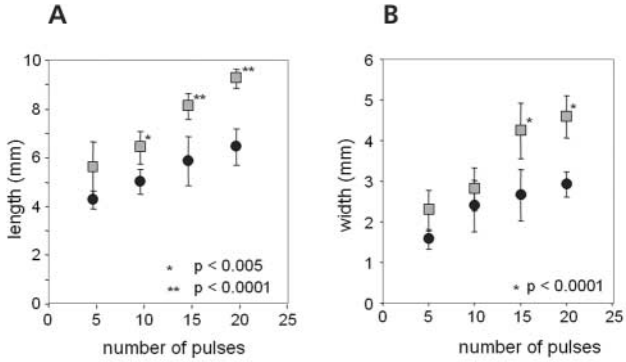

As mentioned previously, LV septal ablation is a potential HIFU application. For the HIFU beam to reach the targeted LV septal region through the RV free wall, it must travel through complex cardiac structures, including the trabeculae carneae, endocardium, and RV cavity. The possibility certainly exists that these structures might alter the lesion sizes because of attenuation and refraction compared with those created in the LV free wall. This study showed that lesions created in the septum through the RV cavity were smaller, but not significantly different, from those created in the LV free wall (Figure 9). Therefore, our results show the feasibility of producing septal lesions through the RV free wall, and they also show the need for further investigations to clarify how exposure levels may need to be adjusted to achieve the desired lesion sizes.

Tissue Temperature Studies

The final general factor we investigated was the effect of tissue temperature on lesion parameters. Tissue temperature is a relevant factor in determining the size of the lesion created. Various previous studies have been completed at room temperature.[21,35,36] High-intensity focused ultrasound can affect tissues through thermal, mechanical, and cavitational mechanisms. Because thermal effects are important in determining the size of a lesion, the temperature of the tissue itself is important. We examined the influence of ambient temperatures, specifically typical room temperatures and body temperatures.

Our studies showed that lesions created at a tissue temperature of 37°C were significantly longer than those created at 23°C and significantly wider with 15 and 20 pulses (Figure 10). As expected, these results indicated that tissue temperature had a significant role in determining the size of the lesion and suggested that in vivo temperatures should be used for future ex vivo HIFU studies.

Additional Considerations

To have controlled exposure during end diastole, the HIFU pulse exposure needs to be synchronized with the ECG. We considered 0.3 seconds to be the longest clinically practical HIFU pulse durations capable of delivering HIFU when the cardiac wall motion was minimal. Even within this short period, a given location within the in vivo myocardium has been shown to move slightly.[26]

Conclusions

High-intensity focused ultrasound creates well-demarcated lesions in ex vivo cardiac muscle without damaging intervening or distal myocardial tissue. The size of the HIFU lesions depends on focal depth, total exposure time, pulse-to-pulse interval, and initial tissue temperature.

Lesion formation in the moving heart can be achieved by intermittent delivery of ultrasonic energy synchronized by ECG triggering. We showed that, for certain clinically important exposure parameters, the lesion size in ex vivo tissue depends strongly on the total exposure time in the range of 0.4 to 2.0 seconds but does not depend strongly on pulse duration in the range of 200 to 300 milliseconds. This is relevant for future clinical applications in which the duration of end diastole may vary according to the heart rate. We also showed that, for a constant total exposure, the lesion width depends strongly on the pulse-to-pulse interval in the range of 0.8 to 4.0 seconds, and the lesion width and length depend strongly on the initial tissue temperature in the range of 23°C to 37°C.

We currently are conducting computer simulations to clarify the importance of these effects and to assess the potential advantages of adjusting focal depth in conjunction with myocardial movement. Guidance for such repositioning could come from ultrasonic images obtained with a diagnostic transducer centrally located within an HIFU array. Furthermore, our computer simulations will allow us to consider separately the contributions of absorption (ie, energy deposition), heat flow, and temperature history to the formation of lesions.[37] These simulations will require future in vivo experiments to show the limitations imposed by the thermodynamics of the ultrasound-tissue interaction.

The initial studies described here indicate strongly that HIFU can potentially provide an effective, noninvasive method for ablating tissues in the treatment of many cardiac ventricular diseases. However, additional research is required for future noninvasive clinical applications, especially in vivo studies, to better understand effects of HIFU on tissues in the path between the transducer and the focal region.

References

1. Miller JM, Zipes DP. Ablation therapy for cardiac arrhythmias. In: Zipes DP, Libby P, Bonow RO, Braunwald E (eds). Braunwald's Heart Disease: A Textbook of Cardiovascular Medicine. 7th ed. Oxford, England: Elsevier Saunders; 2004:739–753.
2. Wynne J, Braunwald E. Hypertrophic cardiomyopathy. In: Zipes DP, Libby P, Bonow RO, Braunwald E (eds). Braunwald's Heart Disease: A Textbook of Cardiovascular Medicine. 7th ed. Oxford, England: Elsevier Saunders; 2004:1677–1681.
3. Swarup V, Morton JB, Arruda M, Wilber DJ. Ablation of epicardial macroreentrant ventricular tachycardia associated with idiopathic nonischemic dilated cardiomyopathy by a percutaneous transthoracic approach. J Cardiovasc Electrophysiol 2002; 13:1164–1168.
4. Maron BJ, Dearani JA, Ommen SR, et al. The case for surgery in obstructive hypertrophic cardiomyopathy. J Am Coll Cardiol 2004; 44:2044–2053.
5. Lynn JG, Zwemer RL, Chick AJ, Miller AG. A new method for the generation and use of focused ultrasound in experimental biology. J Gen Physiol 1942; 26:179–193.
6. Fry WJ, Barnard JW, Fry FJ, Krumins RF, Brennan JF. Ultrasonic lesions in the mammalian central nervous system. Science 1955; 122:517–518.
7. Fry FJ. Precision high-intensity focused ultrasonic machines for surgery. Am J Phys Med 1958; 37:152-156.
8. Fry WJ, Mosberg WH, Barnard JW, Fry FJ. Production of focal destructive lesions in the central nervous system with ultrasound. J Neurosurg 1954; 11:471–478.
9. Chaussy C, Thuroff S. High-intensity focused ultrasound in prostate cancer: result after 3 years. Mol Urol 2000; 4:179–182.
10. Coleman DJ, Silverman RH, Iwamoto T, et al. Histopathologic effects of ultrasonically induced hyperthermia in intraocular malignant melanoma. Ophthalmology 1988; 95:970–981.
11. Hynynen K, Pomeroy O, Smith DN, et al. MR imaging-guided focused ultrasound surgery of fibroadenomas in the breast: a feasibility study. Radiology 2001; 219:176–185.
12. Nakamura K, Baba S, Saito S, Tachibana M, Murai M. High-intensity focused ultrasound energy for benign prostatic hyperplasia: clinical response at 6 months to treatment using Sonablate 200. J Endourol 1997; 11:197–201.
13. ter Haar G. Ultrasound focal beam surgery. Ultrasound Med Biol 1995; 21:1089–1100.
14. Vallancien G, Harouni M, Guillonneau B, Veillon B, Bougaran J. Ablation of superficial bladder tumors with focused extracorporeal pyrotherapy. Urology 1996; 47: 204–207.
15. Wu F, Chen WZ, Bai J, et al. Pathological changes in human malignant carcinoma treated with high-intensity focused ultrasound. Ultrasound Med Biol 2001; 27:1099–1106.
16. Sanghvi NT, Foster RS, Bihrle R, et al. Noninvasive surgery of prostate tissue by high intensity focused ultrasound: an updated report. Eur J Ultrasound 1999; 9:19–29.
17. Sliwa JW, Vaska M, Podmore JL, et al, inventors; Epicor Medical, Inc, assignee. Methods and devices for ablation. US patent 6 689 128. February 10, 2004.
18. Meininger GR, Calkins H, Lickfett L, et al. Initial experience with a novel focused ultrasound ablation system for ring ablation outside the pulmonary vein. J Interv Card Electrophysiol 2003; 8:141–148.
19. Kluiwstra JU, Zhang Y, VanBaren P, Strickberger SA, Ebbin ES, Cain CA. Ultrasound phase arrays for noninvasive myocardial ablation: initial studies. In: Proceedings of the IEEE Ultrasonics Symposium, Seattle, WA. Piscataway, NJ: Institute of Electrical and Electronics Engineers; 1995: 1605–1608.
20. Kluiwstra JU, Tokano T, Davis J, Strickberger SA, Cain CA. Real time imaging guided high intensity focused ultrasound for myocardial ablation: in vivo study. In: Proceeding of the IEEE Ultrasonics Symposium; Toronto, Ontario, Canada. Piscataway, NJ: Institute of Electrical and Electronics Engineers; 1997:1327–1330.
21. Lee LA, Simon C, Bove EL, et al. High-intensity focused ultrasound effect on cardiac tissue: potential for clinical application. Echocardiography 2000; 17:563–566.
22. Sanghvi NT, Fry FJ, Zaitsev A, Olgiu J. Cardiac ablation using high intensity focused ultrasound: a feasibility study. In: Proceedings of the IEEE Ultrasonics Symposium; Toronto, Ontario, Canada. Piscataway NJ: Institute of Electrical and Electronics Engineers; 1997:1323–1326.
23. Smith NB, Hynynen K. The feasibility of using focal ultrasound for transmyocardial revascularization. Ultrasound Med Biol 1998; 24:1045–1054.
24. Strickberger SA, Takano T, Kluiwstra JA, Morady F, Cain C. Extracardiac ablation of the canine atrioventricular junction by use of high-intensity focused ultrasound. Circulation 1999; 100:203–208.
25. Otsuka R, Fujikura K, Hirata K, et al. In vitro ablation of cardiac valves using high-intensity focused ultrasound. Ultrasound Med Biol 2005; 31:109–114.
26. Tridandapani S, Fowlkes JB, Rubin JM. Echocardiography-based selection of quiescent heart phases. J Ultrasound Med 2005; 24:1519–1526.
27. Silverman RH, Vogelsang B, Rondeau MJ, Coleman J. Therapeutic ultrasound for the treatment of glaucoma. Am J Ophthalmol 1991; 111:327–337.
28. Robinson RA. Performance evaluation of a digital readout hyperthermia range ultrasonic wattmeter. IEEE Trans Sonics Ultrasonics 1984; 31:467–472.
29. Muratore R. A history of Sonocare CST: the first FDA-approved HIFU device. In: Clement GT, McDonnald NJ, Hynynen K (eds). Therapeutic Ultrasound: Fifth International Symposium on Therapeutic Ultrasound. New York, NY: AIP; 2006:508–512.

30. Muratore R, Kalisz A, Ramachandran SN, et al. Assessment of HIFU-induced changes in cardiac tissue acoustic properties. Ultrason Imaging 2004; 26:43.

31. Damianou CA, Sanghvi NT, Fry FJ, Maass-Moreno R. Dependence of ultrasonic attenuation and absorption in dog soft tissues on temperature and thermal dose. J Acoust Soc Am 1997; 102:628–634.

32. Kennedy JE. High-intensity focused ultrasound in the treatment of solid tumours. Nat Rev Cancer 2005; 5:321–327.

33. Antman EM, Braunwald E. ST-elevation myocardial infarction: pathology, pathophysiology, and clinical features. In: Zipes DP, Libby P, Bonow RO, Braunwald E (eds). Braunwald's Heart Disease: A Textbook of Cardiovascular Medicine. 7th ed. Oxford, England: Elsevier Saunders; 2004:1145–1150.

34. Lewin PA, Bjorno L. Acoustic pressure amplitude thresholds for rectified diffusion in gaseous microbubbles in biological tissue. J Acoust Soc Am 1981; 69:846–852.

35. Malcolm AL, ter Haar GR. Ablation of tissue volumes using high intensity focused ultrasound. Ultrasound Med Biol 1996; 22:659–669.

36. Miller NR, Bamber JC, ter Haar GR. Imaging of temperature-induced echo strain: preliminary in vitro study to assess feasibility for guiding focused ultrasound surgery. Ultrasound Med Biol 2004; 30:345–356.

37. Muratore R, Lizzi FL, Ramachandran SN, Engel D, Homma S, Marboe CC. Control of the size and shape of myocardial lesions produced by HIFU. In: Proceedings of the Second International Symposium on Therapeutic Ultrasound. Seattle, WA: University of Washington; 2003:323s–329s.